2011 International Nuclear Atlantic Conference - INAC 2011
Belo Horizonte, MG, Brazil, October 24-28, 2011
ASSOCIAÇÃO BRASILEIRA DE ENERGIA NUCLEAR - ABEN
***ISBN:* 978-85-99141-04-5**

X-RAY COMPUTED MICROTOMOGRAPHY AS A TOOL FOR THE COMPARATIVE MORPHOLOGICAL CHARACTERIZATION OF *PROCERATOPHRYS BIGIBBOSA* SPECIES

Francielle da Silva Ahmann[1], Ivan Evseev[1], Manoela Guimarães Ferreira da Paz[1], Rodrigo Lingnau[1], Ievgeniia Ievsieieva[2], Joaquim T. de Assis[2], Haimon D. L. Alves[3]

[1] Universidade Tecnológica Federal do Paraná
Campus Francisco Beltrão
Linha Santa Bárbara, s/n
85601-970 Francisco Beltrão, PR
fran.ahmann@hotmail.com, evseev@utfpr.edu.br,
manoellaguimaraes@hotmail.com, rodrigolingnau@utfpr.edu.br

[2] Instituto Politécnico
Universidade do Estado do Rio de Janeiro
Rua Alberto Rangel, s/n
28630-050 Nova Friburgo, RJ
ievsieieva@iprj.uerj.br, joaquim@iprj.uerj.br

[3] PEN/COPPE/UFRJ
Centro de Tecnologia
Av. Horácio Macedo, 2030
Cidade Universitária, Ilha do Fundão
21941-914 Rio de Janeiro, RJ
haimon.dlafis@gmail.com

ABSTRACT

The *Proceratophrys bigibbosa* species group is characterized by the presence of postocular swellings and absence of hornlike palpebral appendages. A new member of this group was described recently from southern Brazil: *Proceratophrys brauni*. Its body size is between the smaller *Proceratophrys avelinoi* and the larger *Proceratophrys bigibbosa* species, both living in the same region. As the external appearance of these three members of the group is very similar to each other, it is interesting to discover a specific morphological categorization through internal characteristics, such as the cranium's proportions. In this paper, we report the preliminary results for comparative cranium's morphological characterization of *Proceratophrys bigibbosa* species from Brazil using the X-ray computed Microtomography technique through Skyscan 1174 system. Five samples of each three species, i.e., fifteen samples in total, were scanned. The tomographic slice images were reconstructed by SkyScan software. Then, these 2D images were used to create the cranium's models by 3D DOCTOR software. The main result is that some visible differences in the cranium's proportions of the species were observed.

1. INTRODUCTION

In this work, we used the X-ray microtomography (μCT) [1,2] as a tool for the morphological analysis of a frog cranium. Three species of the *Proceratophrys bigibbosa* group in the family Cycloramphidae [3] were studied. This group is characterized by the presence of postocular swellings and large marginal tubercles on eyelids, and absence of hornlike palpebral appendages [3]. The three analyzed species, *P. avelinoi*, *P. bigibbosa* and *P. brauni*

are distributed along rocky and/or muddy streams in south Brazil, Argentina and Paraguay [4,5].

It is quite possible that due to the morphological and acoustical similarity of the species a number of confusion in the identification of some specimens from this *P. bigibbosa* group has been occurred years ago. Also recently, due to more fieldwork done in searching for these frogs, some areas of "sympatry" (localities with overlapping occurrence of two or more species of *P. bigibbosa* group) have been reported [3,5]. Therefore, as the external appearance of these three members of the group is very similar to each other, and the existing museum identification is somewhat doubtful, it is interesting to discover a specific morphological categorization through internal characteristics, such as the cranium's proportions.

Several years ago, the most common technique to study the skeleton structure was based on complete removal of the skin and musculature [6,7]. Alternatively, the so-called "diafanization" could be used. It consists in clearing whole specimens, and staining bones and cartilages, normally used with small vertebrates, including also studies of bone development [8]. The μCT permits both the skeleton visualization with the bones on its natural position, like the second method, and to measure straightforwardly the bones geometry, like the first one. The great advantage of this work is that none of the studied samples were destroyed, or changed.

2. MATHERIALS AND METHODS

2.1. The Frog Samples

The specimens of *P. bigibbosa*, *P. brauni* and *P. avelinoi* were collected in Brazil and Argentina. In Brazil, the origin of specimens is from the municipalities of Ponte Serrada and Lebon Régis in Santa Catarina State, as well as from Altamira do Paraná and Fazenda Rio Grande in Paraná State. In Argentina, the specimens were acquired from Garuape-mí, Departamento Eldorado, Misiones.

Figure 1. Typical specimens (from left to right) of *P. bigibbosa*, *P. brauni*, and *P. avelinoi*.

After being caught, all specimens were sacrificed using 30% alcohol and then covered with 10% formalin as fixative, and deposited in 70% alcohol definitively for the museum collection. Fig.1 shows the representative specimens of *Proceratophrys bigibbosa*, *Proceratophrys brauni* and *Proceratophrys avelinoi* species. It can be seen that the external morphology of three members of the group is very similar to each other, except for the dimensions.

2.2. SkyScan 1174 Tomograph

The frogs were scanned with SkyScan 1174 [9] compact micro-CT system operated at 50kV, 800μA (40W power) with 0.25mm Al filter (Fig.2). During the data acquisition, the turntable rotation was fixed to 1˚ step. For each specimen, 360 radiographic images from the SkyScan 1174 1.3 megapixel X-ray camera were binarized and stored in the computer. The pixel size on the camera was 41.23μm. Due to the cone beam optical magnification, it corresponds to 33.28μm on the object plane. At these conditions, it took approximately 20min to acquire the full set of CT projections for each specimen.

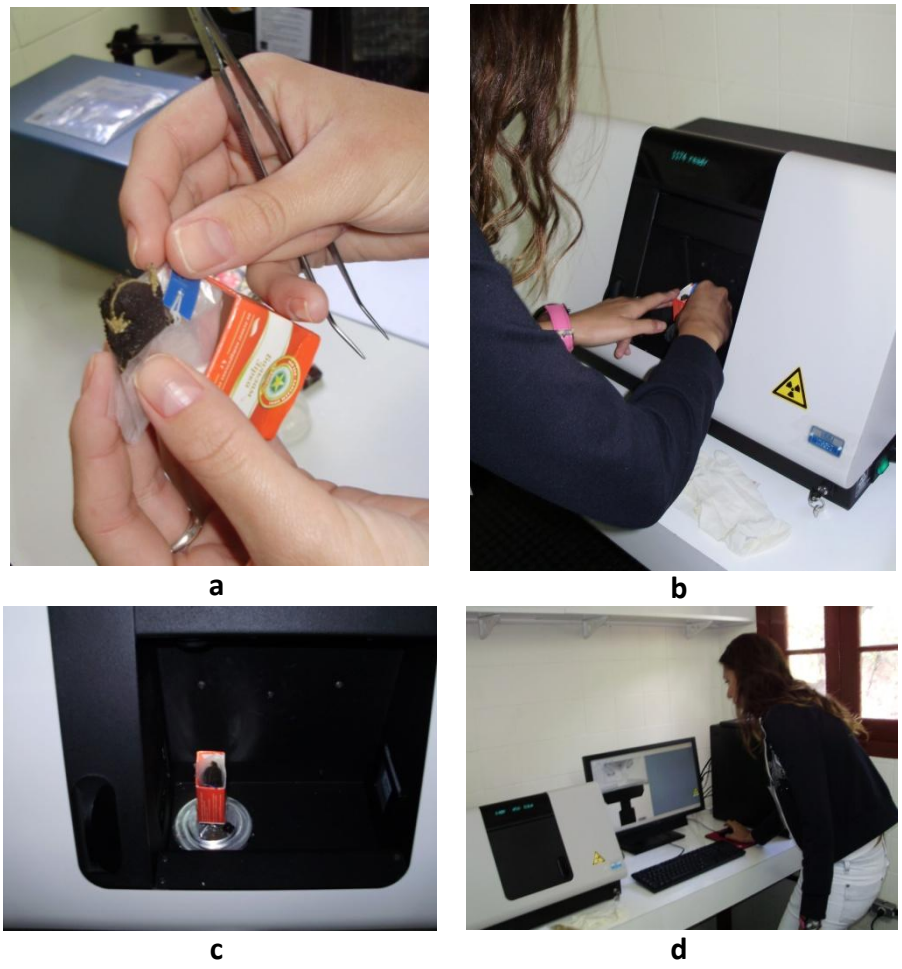

Figure 2. Step by step frog scanning by SkyScan 1174: Fixation in the cardboard (a), positioning on the turntable (b, c) and scanning (d).

A cardboard box was used to fix specimens onto the turntable (Fig.2). It was a critical stage of the study, because the turntable rotation could provoke small displacements of the scanned object. Unfortunately, as a result two blurred 3D reconstructions of *P. avelinoi* were achieved.

The 2D 1024×1024 pixel CT slices were reconstructed using NRecon 1.6.0.3 code. On this stage, the area of interest (i.e. the region where the cranium appears on the radiographic images) was selected to avoid the computer treatment of useless information. In addition, the convenient threshold was slightly adjusted for reconstruction of only the bone component of the specimen according to the aim of the analysis.

Then, the 3D cranium images were rendered from 2D CT slices using the 3D DOCTOR code. These images were used both for the visual qualitative analysis and for quantitative measurements of cranium's geometrical proportions.

2.3. PCA Analysis

In general, the Principal Component Analysis (PCA) is a multivariate technique that analyzes a data table in which observations are described by several inter-correlated quantitative dependent variables [10]. Thus, it is widely used in biological studies [11,12]. In particular, PCA has already been used for the frog's cranium characterization [13,14].

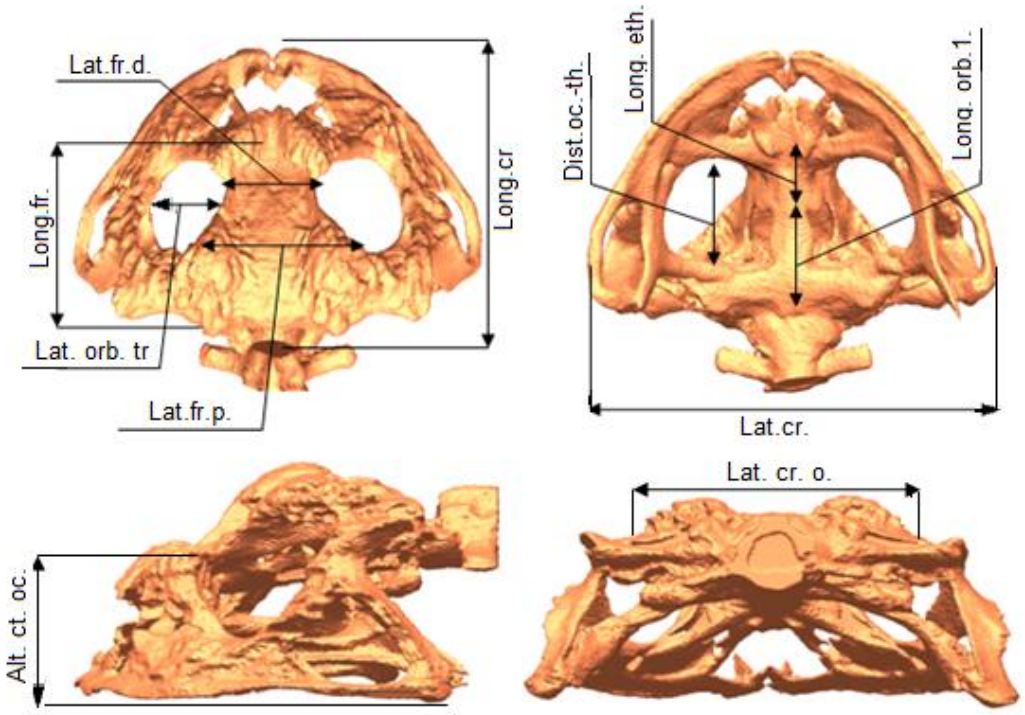

Figure 3. The scheme of cranium measurements

In this work, we took the osteological characteristics from 3D μCT cranium images using work [14] as the instance. The scheme of cranium measurements is shown by Fig.3, and the abbreviation used for notations are expressed by Table 1. Then, the experimental data were treated by MINITAB® statistical software [15].

Table 1. The notations used on Fig.3 to markup the cranium properties.

Characteristic(in *Latin*):	**Abbreviators:**
Latitudo cranii	Lat. cr.
Latitudo cranii ad ossi otici	Lat. cr. o.
Latitudo orbis (directio transversalis)	Lat. orb. tr.
Latitudo ossis frontoparietalis (pars dista-lis)	Lat. fr. d.
Latitudo ossis frontoparietalis (pars proxi-malis)	Lat. fr. p.
Longitudo ossis frontoparietalis	Long. fr.
Longitudo cranii	Long. cr.
Longitudo ossis ethmoidale	Long. eth.
Latitudo orbis (directio longitudinalis)	Lat. orb. l.
Altitudo cranii (margo anterior oculi)	Alt. ct. oc.
Distantio foramen occipitale – ossis ethmoidale terminum proximalis	Dist. oc.-th.

3. RESULTS AND DISCUSSION

3.1. Visual Qualitative Analysis

The main result of this work is that it has been possible to detect some morphological differences of the three species through a visual qualitative analysis of the cranium images. This could be very useful to distinguish specimens from collections when there are doubts about its identification.

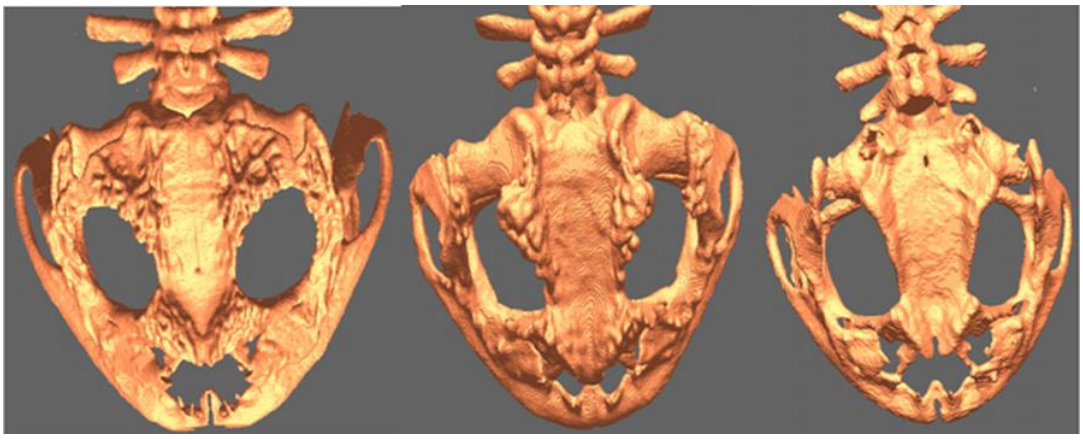

Figure 4. The orthogonal projection of the cranium 3D images in the dorsal view. From left to right: *P. bigibbosa*, *P. brauni*, and *P. avelinoi.*

In a frontal view, for example, there are obvious differences in the projection of tubercles above the ocular socket between *P. brauni* and *P. bigibbosa*, being much more apparent in *P. brauni*. In a dorsal view (see Fig.4), it could be observed that all the region of the frontal parietal bone, including its crest lateral, in *P. avelinoi* is smoother than for others two species. In addition, a bigger projection of the parietal crest reaching the squamosal could be observed for *P. bigibbosa.*

3.2. PCA Analysis

The dimensions of interest were measured from the orthogonal projections of 3D images, as it shown by Fig.3. It means that, in theory, the accuracy of such measurements could be estimated as one-half of the vóxel size, i.e. about 17μm in our case. In practice, however, the result of each measurement is rather subjective. First, it depends on the 3D image orientation to grab the orthogonal projection. As any cranium does not have a simple geometrical form with an absolute symmetry, it could be done only "by the eye". Second, it depends on the choice of the extreme points on the projection, between which that characteristic is measured. Even in the case of a real cranium, the results are dependent of the observer [13,14].

We have not analyzed this problem in details yet, but for our aim is quite enough to know that such uncertainties are much less than the inter sample variations of measured characteristics. The *P. avelinoi* specimens which 3D images were blurred due to not enough fixations onto the tomographic turntable were excluded from the quantitative analyses. Some basic cranium's properties studied in [14], but for which we had doubts in the measuring procedure basing on our CT reconstructions, were excluded from analysis as well.

The next comment should be done about the statistical dimension and the representative quality of our *Proceratophrys bigibbosa* group sample. If the previous identification was truthful, only five specimens of *P. bigibbosa*, five – of *P. brauni,* and three – of *P. avelinoi* were quantitatively analyzed. It is much less than the common recommendation of minimum 20 specimens to have a reasonable statistical analysis of the differences [13,14]. Another common recommendation of these works is to analyze separately the male and female frog specimens. It was not done in our work because of unknown sex of the available specimens.

Thus, we have to limit the aim of our analysis only to the evaluation of input information obtained with μCT as for further PCA examination and separation of the species in more representative samples. Table 2 gives, in each column, the centered and normalized values of the variables (i.e. the given geometric characteristic of the specimen cranium), while each row corresponds to the observation (i.e. to the specimen) [10-13]:

$$X_{i,j} = \frac{x_{i,j} - \mu_j}{\sigma_j} \tag{1}$$

where $X_{i,j}$ is the dimensionless entry in the *i*-th row and *j*-th column of the numerical data matrix in Table 2, $x_{i,j}$ is the measured value of the *j*-th characteristic for the *i*-th specimen from the Table 2, μ_j is the arithmetic mean of the *j*-th characteristic experimental values ($N_j = N = 13$ is the total number of tabulated specimens):

$$\mu_j = \frac{1}{N_j}\sum_{i=1}^{N_j} x_{i,j} \tag{2}$$

and σ_j is the standard deviation of j-th characteristic measured values:

$$\sigma_j = \sqrt{\frac{1}{N_j(N_j-1)}\sum_{i=1}^{N_j}(x_{i,j}-\mu_j)^2} \tag{3}$$

Such representation obviously shows the dimensionless deviations of each characteristic of each individual specimen from the mean value for the sample, which is used as the reference (i.e. the mean is equal to "0" for each column), normalized by the characteristic standard deviation (i.e. the standard deviation is equal to "1" for each column).

In the hypothetical situation of all the specimens being from the same species, and the individual specimen proportions in this subspecies are normally distributed, the histogram of values in each column evidently should give the canonical Gaussian distribution (with a mean of 0 and a standard deviation of 1.). Moreover, due to the centralization and normalization of each column by its standard deviation, all the data from Table 2, i.e. all the characteristics, can be analyzed (from this point of view) simultaneously.

Alternatively, for a mixture of different subspecies, one can expect some deviations from the canonical Gaussian distribution, at least in the standard deviation value.

Table 2. The centered and normalized cranium geometrical characteristics.

Specie	Long.cr.	Lat.fr.p.	Lat.orb.tr.	Long.fr.	Lat.fr.d.	Lat.cr.	Dist.oc.-th.	Long.eth.	Long.orb.	Alt.ct.oc.	Lat.cr.o.
Proceratophrys bigibbosa:											
ROL332	0.68	0.82	1.41	0.81	0.69	1.08	1.01	0.35	1.07	-0.14	1.49
ROL397	-0.58	-0.87	-0.04	-1.61	-0.80	-0.98	0.47	-0.75	-0.99	-0.14	-0.65
ROL571	0.26	0.58	0.92	0.00	-0.21	0.32	-0.33	0.72	0.82	-0.71	0.23
ROL572	0.79	0.58	0.68	0.46	0.69	0.62	0.74	0.35	1.07	0.23	0.99
ROL574	0.68	1.30	0.68	1.61	0.69	1.77	1.01	0.72	1.59	2.11	1.12
Proceratophrys avelinoi:											
DB1984	0.36	-0.27	-0.04	-0.23	0.39	-0.06	-0.06	-0.20	0.04	-0.52	-0.90
DB2370	-1.64	-1.48	-1.48	0.12	-2.00	-1.44	-0.86	-0.75	-0.48	-1.83	-1.91
MHNCI3398	-1.64	-0.63	-1.48	0.12	-1.70	-0.91	0.47	-1.48	-0.74	0.23	0.36
Proceratophrys brauni:											
k778	0.68	0.21	0.92	-0.35	0.39	0.55	1.54	-0.20	0.30	0.79	-0.02
k779	0.26	0.94	-0.76	0.00	0.99	-0.29	-0.06	-0.01	-0.99	0.79	-0.02
k780	1.63	1.06	0.44	0.92	1.29	0.93	-1.13	2.55	0.56	-0.14	0.86
ROL331	-1.11	-1.84	-1.48	-2.19	-0.21	-1.44	-1.93	-0.75	-1.77	-1.27	-1.28
ROL397	-0.37	-0.39	0.20	0.35	-0.21	-0.14	-0.86	-0.56	-0.48	0.61	-0.27

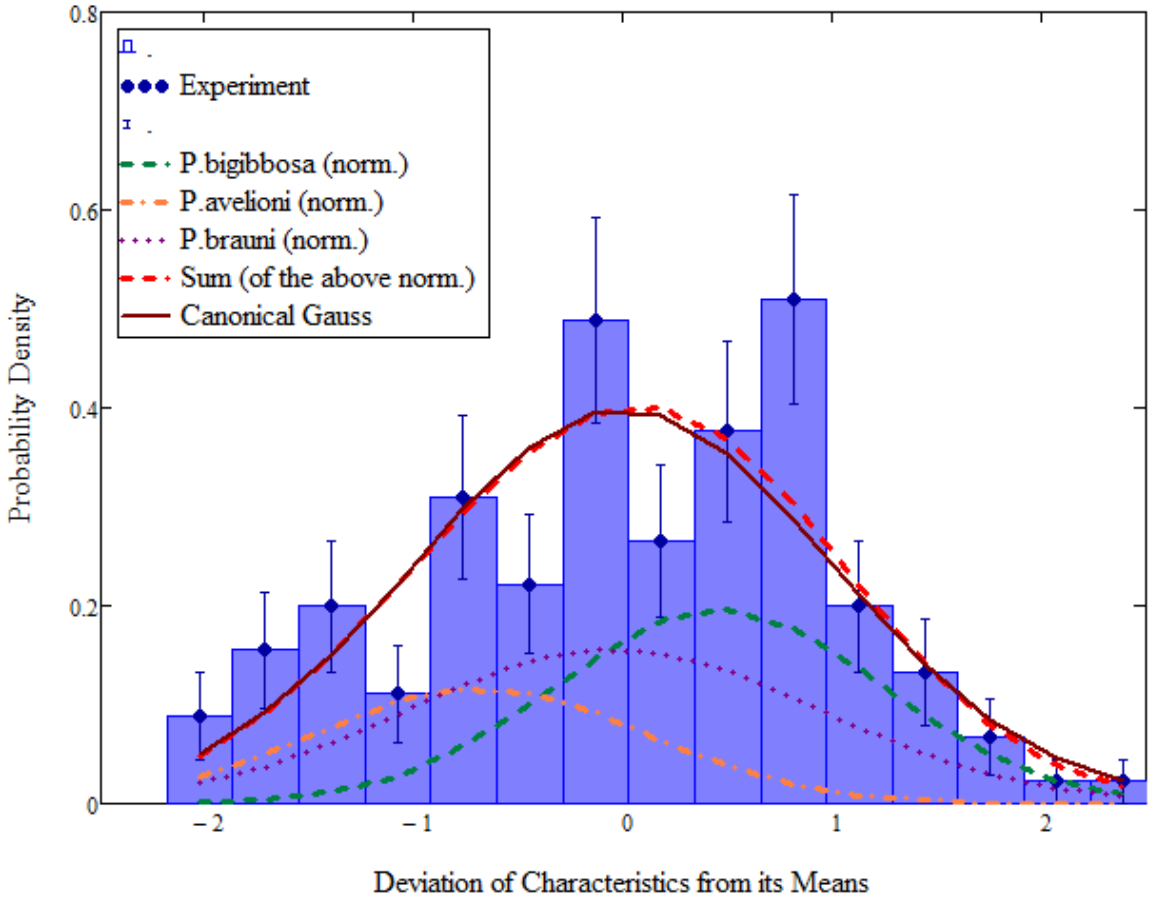

Figure 5. The distribution of deviations in Table 2 (histogram in blue), the Gaussian distributions with experimental parameters for each subspecies, the weighted sum of these distributions (red dashed curve), and the canonic Gaussian distribution (dark brown solid curve).

The real situation is shown by Fig.5. There is no huge disagreement of the deviation distribution with the canonical Gaussian. It is interesting to note that if we trust in museum classification and extract the mean and standard deviation separately for each species from the table, the results will be: $\mu = 0.462$, -0.685, and -0.05; and $\sigma = 0.781$, 0.787, and 0.98 correspondently. Naturally, it is a reflection of the species character dimensions (Fig.1). Now, if then calculate the weighted sum of corresponding Gaussian distributions, the result (the red dashed curve on Fig.5) will practically coincide with the canonical Gaussian distribution (dark brown solid curve). It means that by tacking in consideration the species character dimensions, at least in such simple way we could not make better the agreement of the normal distribution prediction with the experimental data.

The last conclusion is better illustrated by Q-Q plot [16] on Fig.6, where some disagreement is quite visible. Of cause, it could be a simple effect of the "poor" sample statistic. From the other side, such analysis "in overage" could mask a great difference in a particular characteristic. Thus, it is interesting to find out if a few characteristics are responsible for the main part of interspecies deviation.

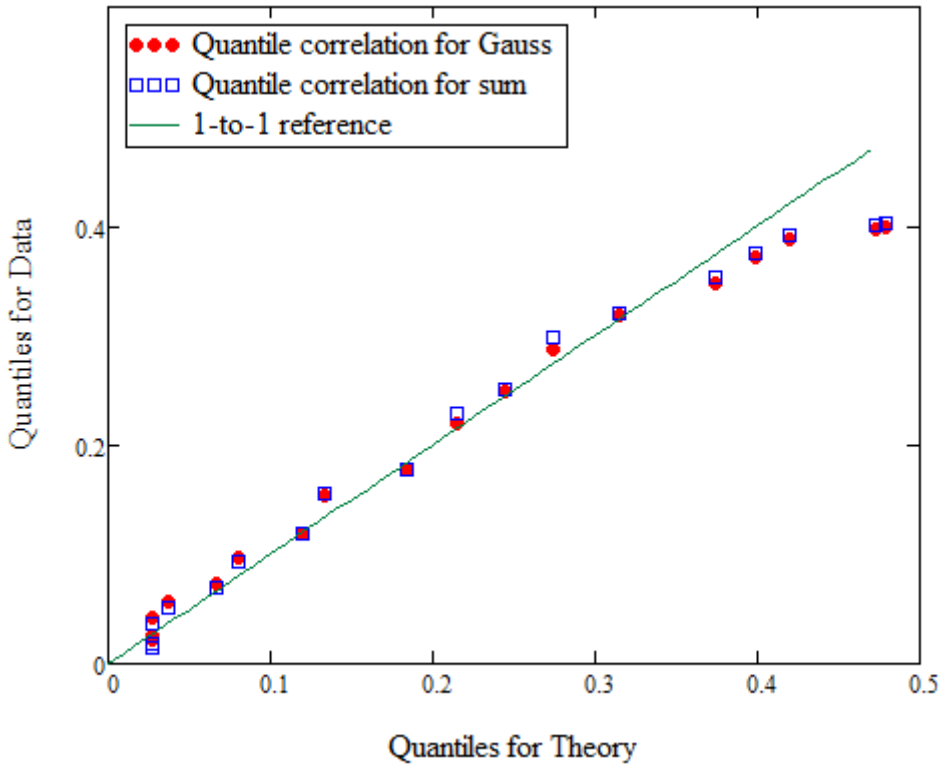

Figure 6. The Q-Q Plot for experimental data distribution versus canonical Gaussian (red points), and the weighted sum of the normal distribution (blue open squares).

The distributions of principal component eigenvalues and cumulative variance show (Fig.7) that the first two principal components are responsible for more than 80% of inter-specimens relative variations [10-12]. Thus, it is it is a good idea to limit the analysis only by the 1st and 2nd principal components (PC).

Fig.8 shows the data from Table 2 as 1st and 2nd PC plot. It could be seen that the first five points for *P. bigibbosa* are concentrated mainly in the left part of the plot: in contrast, the next three points for *P. avelinoi* are concentrated exclusively in the right part of the plot; and the last five points for *P. brauni* are distributed more or less uniformly.

The received loadings for the craniums characteristics into the 1st and 2nd PC are tabulated in Table 3. While the contributions of all the characteristics into the 1st PC are distributed more or less consistently, the loadings into 2nd PC are rather different.

Table 3. The PCA Loadings.

Characteristic:	Long.cr.	Lat.fr.p.	Lat.orb.tr.	Long.fr.	Lat.fr.d.	Lat.cr.	Dist.oc.-th.	Long.eth.	Long.orb.	Alt.ct.oc.	Lat.cr.o.
1st PC:	0.33	0.35	0.31	0.28	0.29	0.36	0.20	0.28	0.32	0.24	0.32
2nd PC:	-0.28	-0.01	0.00	0.13	-0.33	0.02	0.61	-0.50	0.08	0.39	0.14

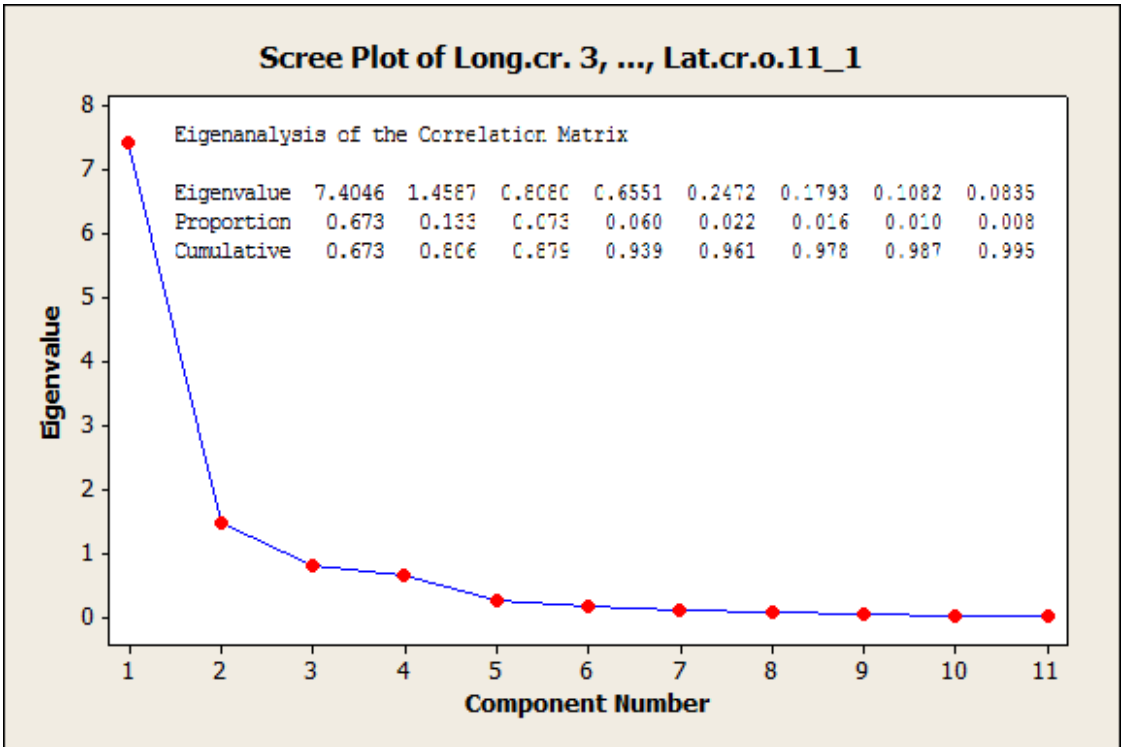

Figure 7. The eigenvalues of principal components.

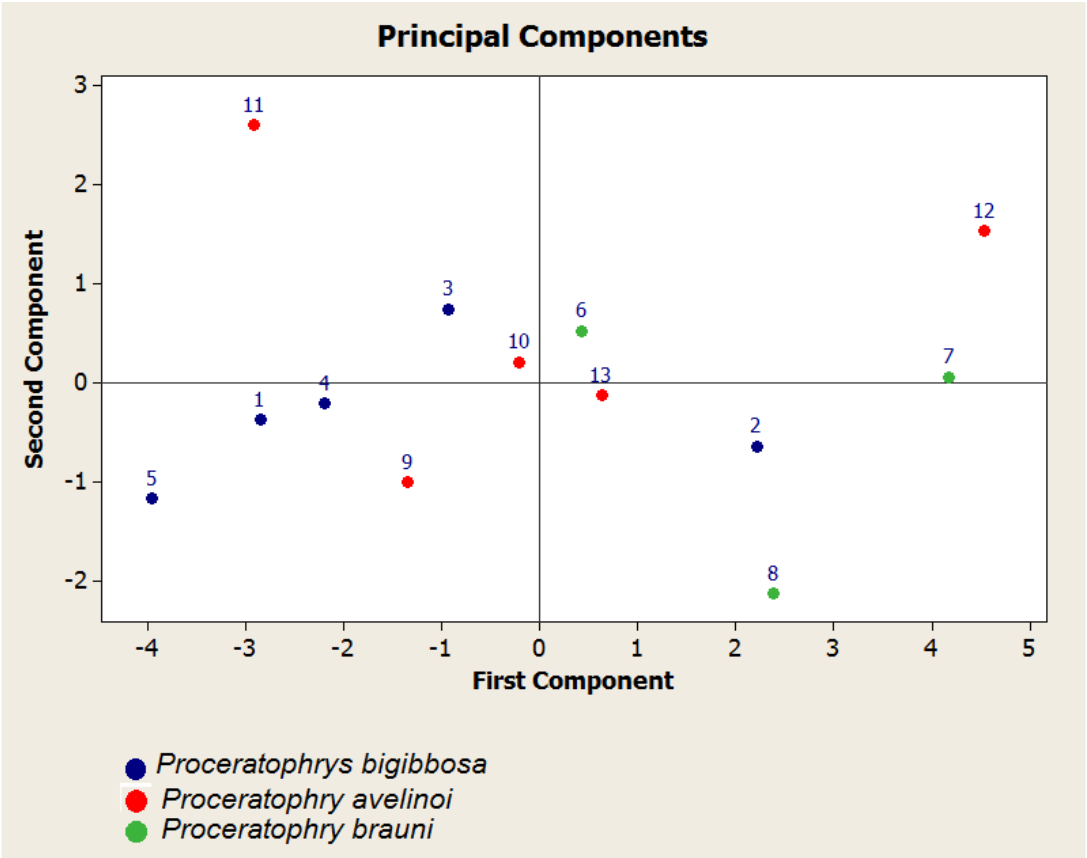

Figure 8. The distribution of specimens on the plot of the 1st and 2nd PC plot.

Comparing this conclusion with the results of qualitative visual analyses one can conclude that the most promised way to separate the *P. bigibbosa*, *P. brauni*, and *P. avelinoi* specimens using μCT in the existing museum collections, as well as the new ones, is to establish some specific geometrical characteristics connected with the obvious osteological differences.

4. CONCLUSIONS

The main result of this work is that some evident differences in the cranium proportions of samples could be observed in the 3D CT reconstructions, obtained within the operation mode of SkyScan 1174 with moderate spatial resolution. It should be noted that SkyScan 1174 permits to work with better spatial resolution. The better spatial resolution, however, has the cost of drastically increasing time for CT image reconstruction and further manipulation. Thus, it make a sense to utilize such regime only if a more detailed information on bone structure than the general cranium analysis is required. Such studies are under consideration now. As for this work, we proved that the frog craniometrical study is viable to do rapidly utilizing μCT. Having in mind the obvious advantages of the method it could be concluded that such analysis is very promising for a large variety of amphibians, and biologic species in general.

ACKNOWLEDGMENTS

The authors are greatly thankful to the Brazilian agencies CNPq, CAPES and "Fundação Araucaria" (Paraná State) for the financial support of this work. We are also thankful to C. E. Conte, D. Baldo, and J. C. Moura-Leite for allowing examination on some specimens of *Proceratophrys* under their care.

REFERENCES

1. A. C. Kak and M. Slaney, *Principles of Computerized Tomographic Imaging*, IEEE Press Inc., N.Y., USA (1988).
2. S. R. Stock, *Micro Computed Tomography: Methodology and Applications*, CRC Press, Boca Raton - FL, USA (2008).
3. A. Kwet, and J. Faivovich, "*Proceratophrys bigibbosa* species group (Anura: Leptodactylidae), with description of a new species", *Copeia*, **2001**(1), pp.203-215 (2001).
4. A. Carosini, P. Pérez., M. L. Ortiz, et al., "Amphibia, Anura, Cycloramphidae, Proceratophrys avelinoi Mercadal de Barrio and Barrio, 1993: distribution extension and distribution map", *Check List*, **6**(2), pp.332-333 (2010).
5. R. R. Santos, P. Colombo, S. B. Leonardi, et al., "Amphibia, Anura, Cycloramphidae, *Proceratophrys bigibbosa* (Peters, 1872) and *Proceratophrys brauni* (Kwet and Faivovich, 2001): distribution extension and new state record", *Check List*, **5**(4), pp.922-925 (2009).
6. J. D. Lynch, "Evolutionary relationships, osteology, and zoogeography of leptodactyloid frogs", *University of Kansas Museum of Natural History Miscellaneous Publication* **53**, pp.1-238 (1971).
7. A. S. Romer, *The vertebrate body*. Second Edition, W. B. Saunders Co. 1955.

8. W. Taylor, G. C Van Dyke, “Revised procedures for staining and clearing small fishes and other vertebrates for bone and cartilage study”, *Cybium*, **9**, pp.107-119 (1985).
9. “SkyScan’s website”, www.skyscan.be (2011).
10. I. T. Jolliffe, *Principal component analysis*. Springer, N.Y., USA (2002).
11. H. Abdi, L. J. Williams, “Principal component analysis”, *Wiley Interdisciplinary Reviews: Computational Statistics*, **2**(4), pp.433–459 (2010).
12. В. М. Ефимов, В.Ю. Ковалева, *Многомерный анализ биологических данных*, РИО Горно-Алтайского госуниверситета, Горно-Алтайск, Россия (2007), in Russian.
13. L.-A. C. Hayek, W. R. Heyer, C. Gascon, “Frog morphometrics: a cautionary tale”, *Alytes*, **18**(3-4), pp.153-177 (2001).
14. Е. М. Писанец, С. Н. Литвинчук, Ю. М. Розанов, et al., “Серые жабы (Amphibia, Bufonidae, *Bufo bufo* complex) предкавказья и Северного Кавказа: Новый анализ проблемы”, *Збірник праць Зоологічного музею*, **№ 40**, сс.87-129 (2008–2009), in Russian.
15. “MINITAB’s Website”, www.minitab.com (2011).
16. R. Gnanadesikan, M. B. Wilk, "Probability plotting methods for the analysis of data", *Biometrika*, **55**(1), pp.1–17 (1968).